

Design and Analysis of Highly Efficient and Reliable Single-Phase Transformerless Inverter for PV Systems

L. Ashok Kumar, N. Sujith Kumar

Abstract—Most of the PV systems are designed with transformer for safety purpose with galvanic isolation. However, the transformer is big, heavy and expensive. Also, it reduces the overall frequency of the conversion stage. Generally PV inverter with transformer is having efficiency around 92%–94% only. To overcome these problems, transformerless PV system is introduced. It is smaller, lighter, cheaper and higher in efficiency. However, dangerous leakage current will flow between PV array and the grid due to the stray capacitance. There are different types of configurations available for transformerless inverters like H5, H6, HERIC, oH5, and Dual paralleled buck inverter. But each configuration is suffering from its own disadvantages like high conduction losses, shoot-through issues of switches, dead-time requirements at zero crossing instants of grid voltage to avoid grid shoot-through faults and MOSFET reverse recovery issues. The main objective of the proposed transformerless inverter is to address two key issues: One key issue for a transformerless inverter is that it is necessary to achieve high efficiency compared to other existing inverter topologies. Another key issue is that the inverter configuration should not have any shoot-through issues for higher reliability.

Keywords—Leakage current, common mode (CM), photovoltaic (PV) systems, pulse width modulation (PWM).

I. INTRODUCTION

DUE to the rapid increase in human population and limitation reserve of natural resources such as coal and fuel, solar power is considered to be better option to meet these challenges since it is naturally available, pollution free and inexhaustible. Besides, with the help of government incentives and decrease in PV module prices, grid-connected PV systems play an important role in distributed power generation. The decrease in cost of PV system, the advancement of power electronics and semiconductor technology and incentives from government strongly encourage the growth of grid-connected PV systems [1].

Grid-connected PV system can be classified into two categories: with and without transformer. Most of the PV systems are designed with transformer for safety purpose with galvanic isolation. Galvanic isolation ensures no injection of DC current into the grid and reduces the leakage current between PV module and grid.

In DC side, high frequency transformer is used whereas bulky low frequency transformer is used in output side of the

inverter. However, the transformer is big, heavy and expensive. Also, it reduces the overall frequency of the conversion stage.

To overcome these problems, transformerless PV system is introduced. It is smaller, lighter, cheaper and higher in efficiency [2], [3]. However, the elimination of the transformer may cause fluctuation of the potential between solar array and the ground which is also known stray capacitance or parasitic capacitance. The value of the stray capacitance depends on the surface of the PV array and grounded frame, distance of PV cell to the module, atmospheric conditions, dust and humidity. This stray capacitance is energized by the fluctuating potential and leads to leakage current. Electrical hazard occurs when a person touches the PV array. Leakage current flows through the person to the ground [4]. Furthermore, DC current will be injected to the grid causing the saturation of the distribution transformer along the grid [5].

This CM ground current will cause an increase in the current harmonics, higher losses, safety problems, and Electro Magnetic Interference (EMI) issues. For a grid-connected PV system, energy yield and payback time are greatly dependent on the inverter's reliability and efficiency, which are regarded as two of the most significant characteristics for PV inverters [6]-[9]. In order to minimize the ground leakage current and improve the efficiency of the converter system, transformerless PV inverters utilizing unipolar PWM control have been presented.

II. OBJECTIVES

The main goal is to design a transformerless inverter with high reliability and maximum efficiency greater than that of presently available configurations by overcoming their problems and to reduce leakage currents. In order to avoid injection of DC current into the grid and to suppress the leakage current within the permissible level, certain converter structures and modulation methods have been proposed. In this paper, a new transformerless topology is modeled, analyzed and validated by simulation.

The main objective of the proposed transformerless inverter is to address two key issues: One key issue for a transformerless inverter is that it is necessary to utilize super junction MOSFETs (CoolMOS) for all switching devices to achieve high efficiency. Another key issue is that the inverter configuration should not have any shoot-through issues for higher reliability.

L. Ashok Kumar is Professor with the Electrical and Electronics Engineering Department, PSG College of Technology, Coimbatore, India (e-mail: lak@eee.psgtech.ac.in).

N. Sujith Kumar is PGET - R&D with the Danfoss Power Electronics Division, Danfoss Industries Pvt. Ltd., Chennai, India (e-mail: sujith@danfoss.com).

III. PROPOSED TOPOLOGY

A. Proposed Topology Features

One key issue for a high efficiency and reliability transformerless PV inverter is that in order to achieve high efficiency over a wide load range it is necessary to utilize super junction MOSFETs for all switching devices. Another key issue is that the inverter should not have any shoot-through issues for higher reliability. In order to address these two key issues, a new inverter topology is proposed for single phase transformerless PV grid-connected systems.

The proposed transformerless PV inverter features:

- 1) High reliability because there are no shoot-through issues.
- 2) Low output ac current distortion as a result of no dead time requirements at every PWM switching commutation instant as well as at grid zero crossing instants.
- 3) Minimized CM leakage current because there are two additional ac side switches that decouple the PV array from the grid during the freewheeling phases.
- 4) All the active switches of the proposed converter can reliably employ MOSFETs since it never has the chance to induce MOSFET body diode reverse recovery.

As a result of the low conduction and switching losses of the super junction MOSFETs, the proposed converter can be designed to operate at higher switching frequencies while maintaining high system efficiency.

B. Proposed Topology Operation

Fig. 1 shows the circuit diagram of the proposed transformerless PV inverter, which is composed of six MOSFET switches (S1–S6), six diodes (D1–D6), and two split ac coupled inductors L1 and L2. The diodes D1–D4 perform voltage clamping functions for active switches S1–S4. The ac side switch pairs are composed of S5, D5 and S6, D6, respectively, which provide unidirectional current flow branches during the freewheeling phases decoupling the grid from the PV array and minimizing the CM leakage current.

Compared to the HERIC topology the proposed inverter topology divides the ac side into two independent units for positive and negative half cycle. In addition to the high efficiency and low leakage current features, the proposed transformerless inverter avoids shoot-through enhancing the reliability of the inverter. The inherent structure of the proposed inverter does not lead itself to the reverse recovery issues for the main power switches and as such super junction MOSFETs can be utilized without any reliability or efficiency penalties.

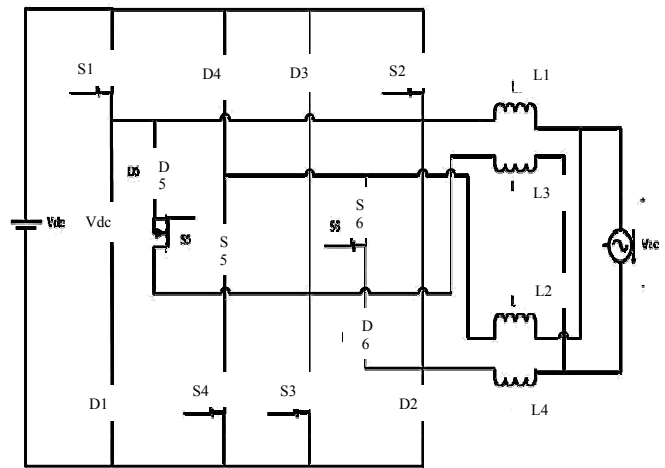


Fig. 1 Proposed transformerless inverter configuration

C. Circuit Operation Analysis

Figs. 2-5 show the four operation stages of the proposed inverter within one grid cycle. In the positive half line grid cycle, the high frequency switches S1 and S3 are modulated by the sinusoidal reference signal $V_{control}$ while S5 remains turned ON. When S1 and S3 are ON, diode D5 is reverse biased, the inductor currents of i_{L01} and i_{L03} are equally charged, and energy is transferred from the dc source to the grid when S1 and S3 are deactivated, the switch S5 and diode D5 provide the inductor current i_{L01} and i_{L03} a freewheeling path decoupling the PV panel from the grid to avoid the CM leakage current. Coupled inductor L2 is inactive in the positive half line grid cycle. Similarly, in the negative half cycle, S2 and S4 are switched at high frequency and S6 remains ON. Freewheeling occurs through S6 and D6.

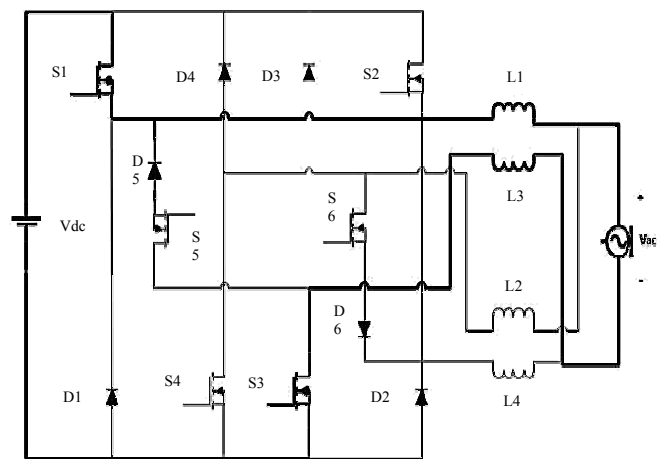


Fig. 2 Active stage of positive half line cycle

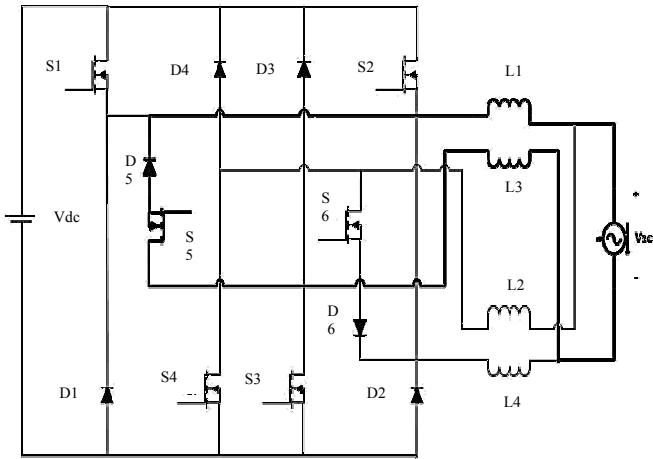


Fig. 3 Freewheeling stage of positive half line cycle

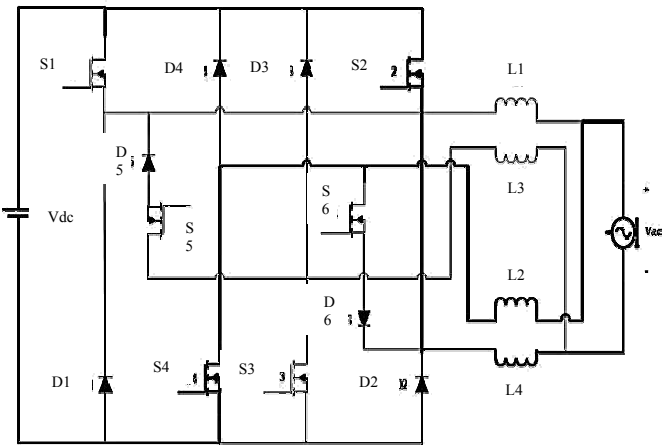


Fig. 4 Active stage of negative half line cycle

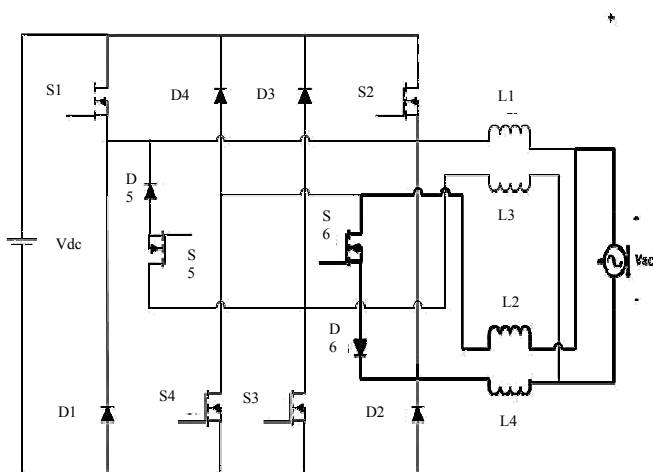


Fig. 5 Freewheeling stage of negative half line cycle

IV. LEAKAGE CURRENT ANALYSIS

A galvanic connection between the ground of the grid and the PV array exists in transformerless grid-connected PV systems. Large ground leakage currents may appear due to the

high stray capacitance between the PV array and the ground [10]-[12]. In order to analyse the ground loop leakage current, Fig. 6 shows a model with the phase output points 1, 2, 3, and 4 modelled as controlled voltage sources connected to the negative terminal of the dc bus (N point).

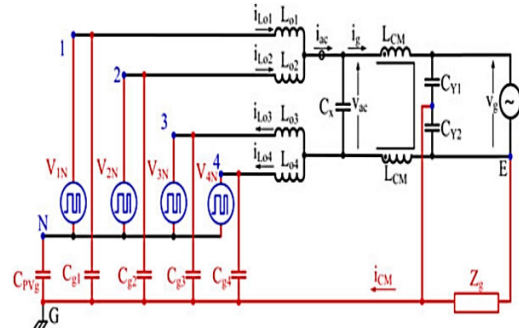


Fig. 6 Leakage current analysis model for the proposed transformerless inverter

Fig. 6 clearly illustrates the stray elements influencing the ground leakage current, which include:

- 1) The stray capacitance between PV array and ground C_{PVg} .
- 2) Stray capacitances between the inverter devices and the ground $C_{g1}-C_{g4}$.
- 3) The series impedance between the ground connection points of the inverter and the grid Z_g . The differential mode (DM) filters capacitor C_x and the CM filter components L_{CM} , C_{Y1} , and C_{Y2} are also shown in the model.

The value of the stray capacitances C_{g1} , C_{g2} , C_{g3} , and C_{g4} of MOSFETs is very low compared with that of C_{PVg} , therefore the influence of these capacitors on the leakage current can be neglected [13]. It is also noticed that the DM capacitor C_x does not affect the CM leakage current. Moreover, during the positive half line cycle, switches S2, S4, and S6 are kept deactivated hence the controlled voltage sources V_{2N} and V_{4N} are equal to zero and can be removed. Consequently, a simplified CM leakage current model for the positive half line cycle is derived as shown in Fig. 7.

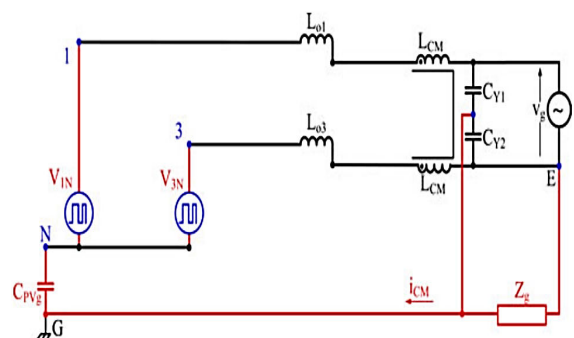


Fig. 7 Simplified CM leakage current analysis model for +ve half-line cycle

With the help of the CM and DM concepts and by introducing the equivalent circuits between N and E, a single

loop mode applicable to the CM leakage current analysis for the positive half line cycle of the proposed transformerless inverter is obtained, as shown in Fig. 7, with (1) and (2)

$$V_{CM} = \frac{V_{1N} + V_{3N}}{2} \quad (1)$$

$$V_{DM} = V_{1N} - V_{3N} \quad (2)$$

A total CM voltage V_{tCM} is defined as (3)

$$V_{tCM} = V_{CM} + V_{DM} \cdot \frac{L_{01} - L_{03}}{2(L_{01} + L_{03})} \\ = \frac{V_{1N} + V_{3N}}{2} + (V_{1N} - V_{3N}) \cdot \frac{L_{01} - L_{03}}{2(L_{01} + L_{03})} \quad (3)$$

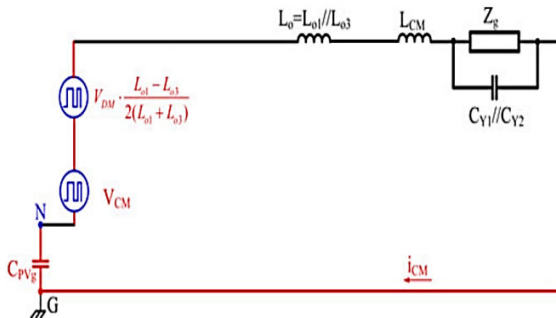


Fig. 8 Simplified single loop CM model for positive half line cycle

It is clear that if the total CM voltage V_{tCM} keeps constant, no CM current flows through the converter. For a well-designed circuit with symmetrically structured magnetics, normally L_{01} is equal to L_{03} . During the active stage of the positive half line cycle, V_{1N} is equal to V_{dc} , while V_{3N} is equal to 0. Hence, the total CM voltage can be calculated as (4)

$$V_{tCM} = \frac{V_{1N} + V_{3N}}{2} + (V_{1N} - V_{3N}) \cdot \frac{L_{01} - L_{03}}{2(L_{01} + L_{03})} = \frac{V_{dc}}{2} \quad (4)$$

During the freewheeling stage of the positive half line cycle, under the condition that S1 and S3 share the dc link voltage equally when they are simultaneously turned OFF, one can obtain (5)

$$V_{1N} = V_{3N} = \frac{V_{dc}}{2} \quad (5)$$

Therefore, the total CM voltage during the freewheeling stage is calculated as (6)

$$V_{tCM} = \frac{V_{1N} + V_{3N}}{2} + (V_{1N} - V_{3N}) \cdot \frac{L_{01} - L_{03}}{2(L_{01} + L_{03})} = \frac{V_{dc}}{2} \quad (6)$$

Equations (4) and (6) indicate that the total CM voltage keeps constant in the whole positive half line cycle. As a result, no CM current is excited. Similarly, during the whole negative half line cycle, the CM leakage current mode is exactly the same as the one during the positive half line cycle the only difference is the activation of different devices. The total CM voltage in the negative half line cycle is also equal to

$V_{dc}/2$. Therefore, in the whole grid cycle the total CM voltage keeps constant, minimizing CM ground leakage current.

V. RESULTS AND DISCUSSION

Fig. 9 shows the proposed transformerless inverter SIMULINK model, which is composed of six MOSFET switches (S1–S6), six diodes (D1–D6), and two split ac coupled inductors L1 and L2. The diodes D1–D4 perform voltage clamping functions for active switches S1–S4. The ac side switch pairs are composed of S5, D5 and S6, D6, respectively, which provide unidirectional current flow branches during the freewheeling phases decoupling the grid from the PV array and minimizing the CM leakage current.

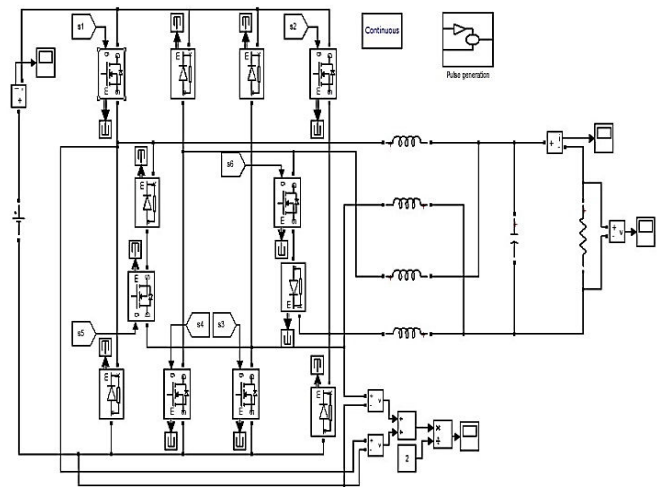


Fig. 9 Proposed transformerless inverter SIMULINK model

A. Filter Design Calculations

Grid frequency $f = 50$ Hz

Cut-off frequency should ≥ 20 times of grid frequency

So, Cut-off frequency $f_0 = 20 \times 50 = 1000$ Hz

$$L = \frac{R_d}{2\pi f_0}$$

$$R_d = 12 \Omega$$

$$L = \frac{12}{2\pi \times 1000} = 1.9 \text{ mH}$$

$$C_b = \frac{1}{2\pi \times 50 \times 12} = 265 \mu\text{F}$$

$$C = 2.5\% \text{ of } C_b = 0.025 \times 265 \mu\text{F} = 6 \mu\text{F}$$

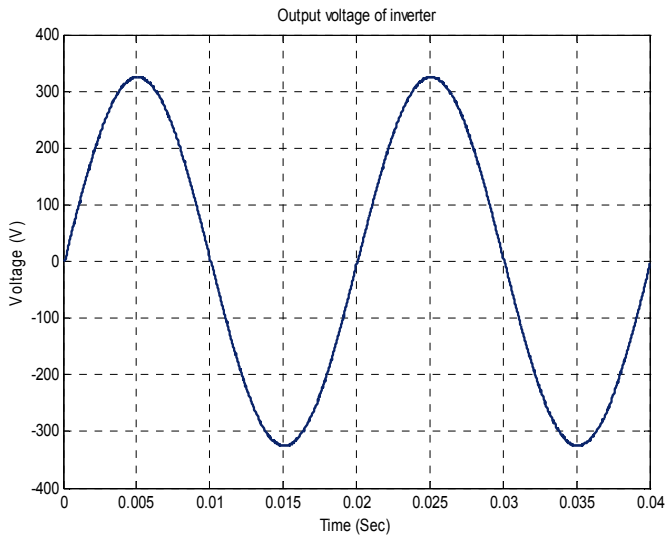


Fig. 10 Output voltage of proposed inverter

Figs. 10 and 11 show the output voltage and output current of proposed transformerless inverter respectively. From the figures the output voltage and output currents are pure sinusoidal shape in nature with the use of very small values of filter elements. As the voltage and currents are in sinusoidal in nature the THD is very low which is as shown in Fig. 12.

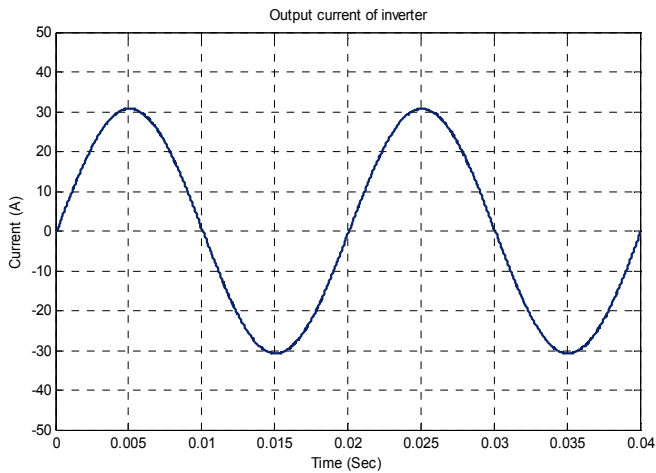


Fig. 11 Output current of proposed inverter

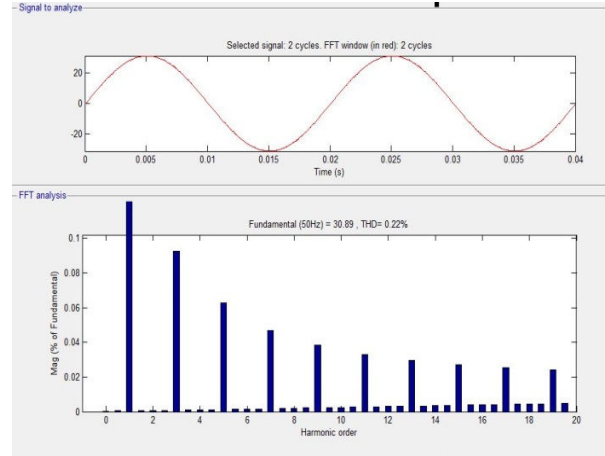


Fig. 12 Output current THD of proposed inverter

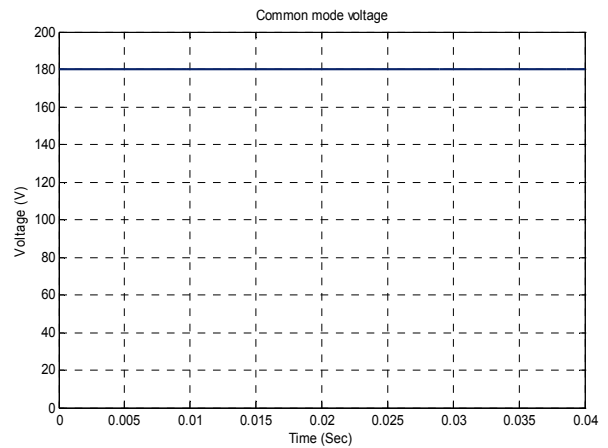


Fig. 13 Common mode voltage of proposed inverter

Fig. 13 shows the common mode voltage of proposed transformerless inverter as a constant voltage of 180V which is half of given input voltage of 360V. Fig. 13 common mode voltage is satisfies (5). As the common mode voltage is kept constant the leakage currents will be less.

VI. CONCLUSIONS

A high reliability and efficiency inverter for transformerless PV grid-connected power generation systems is designed, analysed and simulated. The corresponding simulation results were presented. The main characteristics of the proposed transformerless inverter are summarized as follows: Ultra high efficiency can be achieved over a wide output power range by reliably employing super junction MOSFETs for all switches since their body diodes are never activated. No shoot-through issue leads to greatly enhanced reliability. Low ac output current distortion is achieved because dead-time is not needed at PWM switching commutation instants. Low CM leakage current is present as a result of two additional unidirectional current switches decoupling the PV array from the grid during the zero stages. Higher switching frequency operation is allowed to reduce the output current ripple and the size of

passive components while the inverter maintains high efficiency.

REFERENCES

- [1] M. Calais, J. Myrzik, T. Spooner, V. G. AgeJidis, "Inverters for single phase grid-connected photovoltaic system-an overview," Power Electronics Specialists Conference, Vol. 4, pp. 1995-2000, June 2002.
- [2] M. Calais and V. Agelidis, "Multilevel converters for single phase grid-connected photovoltaic systems, an overview" in IEEE International Symposium on Industrial Electronics, 7-10, pp. 224-229, Jul. 1998.
- [3] N. Jenkins "Photovoltaic systems for small scale remote power supplies" Power Engineering Journal, vol. 9, no. 2, pp. 89-96, Apr. 1995.
- [4] M. Svrzek and G. Sterzinger, "Solar PV Development: Location of Economic Activity" Renewable Energy Policy Report 2005.
- [5] M.J. de Wild-Scholten, E.A. Alsema, E.W. ter Horst, M. Bächler, and V.M. Fthenakis, "A Cost and Environmental Impact Comparison Of Grid-connected Rooftop and Ground Based PV Systems" in 21th European PV Solar Energy Conference, 4-8, pp.1-7, Sep. 2006.
- [6] S. Kjær, J. Pedersen, and F. Blaabjerg, "A review of single phase grid-connected inverters for photovoltaic modules" IEEE Transactions on Industry Applications, vol. 41, no. 5, pp. 1292- 1306, Sep. 2005.
- [7] H. Häberlin "Evolution of inverters for grid-connected PV systems from 1989 to 2000" in 17th European Photovoltaic Solar Energy Conference, 22-26, Oct. 2002.
- [8] M Meinhardt and G. Cramer, "Past, Present and Future of grid-connected Photovoltaic and Hybrid Power Systems" in IEEE Power Engineering Society Summer Meeting., pp. 1283-1288, Jul. 2000.
- [9] M. Calais, J. Myrzik, T. Spooner, and V.G. Agelidis, "Inverters for single phase grid-connected photovoltaic systems an overview" in IEEE 33rd Annual Power Electronics Conference, pp. 1995 – 2000, Jun 2002.
- [10] M. Abella and F. Chenlo, "Choosing the right inverter for grid-connected PV systems" Renewable Energy World, vol. 7, no. 2, pp. 132-147, Mar-Apr. 2004.
- [11] J.M. Carrasco et al. "Power Electronic Systems for the Grid Integration of Renewable Energy Sources: A Survey" IEEE Transactions on Industrial Electronics, vol. 53, no. 4, pp. 1002-1016, Aug. 2006.
- [12] Bo Yang, WuhuaLi, YunjieGu, Wenfeng Cui, and Xiangning He, Improved Transformerless Inverter With Common-Mode Leakage Current Elimination for a Photovoltaic Grid-connected Power System, IEEE transactions on power electronics, vol.27, February 2012.
- [13] Rekioua D., Matagne E. Optimization of photovoltaic power systems: Modelization, Simulation and Control (2012) Green Energy and Technology, 102.